Journal of Hazardous Materials 192 (2011) 1364–1369

Contents lists available at ScienceDirect

Journal of Hazardous Materials

journal homepage: www.elsevier.com/locate/jhazmat

# Effects of engineered nano-titanium dioxide on pore surface properties and phosphorus adsorption of sediment: Its environmental implications

Zhuanxi Luo [a], Zhenhong Wang [a,b], QunShan Wei [a], Changzhou Yan [a,*], Feng Liu [a]

[a] Key Laboratory of Urban Environment and Health, Institute of Urban Environment, Chinese Academy of Sciences, Xiamen 361021, China
[b] Zhangzhou Normal University, Department of Chemistry and Environment Sciences, Zhangzhou 363000, China

ARTICLE INFO

*Article history:*
Received 14 February 2011
Received in revised form 26 May 2011
Accepted 18 June 2011
Available online 5 July 2011

*Keywords:*
Engineered nanoparticles
Fractal dimension
Porosity
Adsorption

ABSTRACT

Understanding the environmental safety and human health implications of engineered nanoparticles (ENPs) is of worldwide importance. As an important ENPs, engineered nano-$TiO_2$ (Enano-$TiO_2$) may have been substantially deposited in aquatic sediments because of its widely uses. Sediment pore surface properties would be thus significantly influenced due to the large surface area of Enano-$TiO_2$. In this study, Enano-$TiO_2$ was found to greatly impact on sediment pore surface properties. The attachment of Enano-$TiO_2$ particles to sediment surfaces enhanced markedly BET specific surface area and t-Plot external specific surface area, and thereby increased sediment phosphorus (P) adsorption maximum ($S_{max}$). Contrarily, the fill of Enano-$TiO_2$ particles into the micropores of sediments could significantly reduce t-Plot micropore specific surface area, and cause slight decrease in sediment P binding energy (K). Clearly, P sorbed in sediment would be easily released because of the decreasing P binding energy of the sediment with elevated Enano-$TiO_2$. Enano-$TiO_2$ would thus cause aggravated endogenous pollution in water if such sediment was re-suspended on disturbance. The results obtained in this study contribute to our increasing knowledge of how to regulate physicochemical behavior of pollutants in sediments under the influences of Enano-$TiO_2$ and/or similar ENPs.



## 1. 1 Introduction

Nanotechnology is advancing rapidly and could soon become a trillion-dollar industry [1]. Consequently, substantial amount of engineered nanoparticles (ENPs) may inevitably enter the environment. Possible risks of ENPs are unintended human health and environmental impacts, which could lead to lack of public acceptance [2]. Therefore, understanding the safety and environmental and human health implications of nanotechnology-based products is of worldwide importance [3–5]. Recently, the potential of harmful effects to the environment and human health by some nanoparticles has been gradually acknowledged [2,6–8]. Studies into the release potential and transport of ENPs indicate that several ENPs actually end up in the aquatic environment with significant quantity [9,10]. ENPs are particles that have at least one dimension between 1 and 100 nm, and are specifically engineered to have unique properties that do not exist in bulk materials with an identical composition [11]. To date, it is still unclear how ENPs influence sediment physicochemical properties that could affect the mobilization of toxic and/or harmful chemicals in sediments. Therefore, knowledge of how ENPs impact on sediment properties is critical.

Engineered Titania nanoparticles (Enano-$TiO_2$) are widely used for applications such as pigments, coatings, sunscreen cosmetic additives, etc. [12–14]. As a result, Enano-$TiO_2$ may inevitably enter the environment, then deposit in aquatic sediments [15–17]. Therefore, such Enano-$TiO_2$ may result in changes in sediment physicochemical properties due to its large surface area and great reactivity [18,19]. To our current knowledge, most researches focused on ecotoxicology of Enano-$TiO_2$ in the aquatic environment [20–22]. Little is known about the effects of Enano-$TiO_2$ on sediment physicochemical properties. Sediment pore surface area is a significant aspect of sediment physicochemical characteristics, and it controls the adsorption and transport of many chemicals in sediments [23]. Hence, the knowledge of how Enano-$TiO_2$ affects sediment pore surface properties is necessary in assessing the environmental risk of this material.

Phosphorus (P) is one of the greatest concerns because it can contribute significantly to eutrophication in aquatic environment [24–27]. Sediment pore surface properties could play critical roles in P adsorption [28]. A recent study indicates that Enano-$TiO_2$ can retard P release from sediment, and thereby improve P adsorption on the sediment, possibly due to the high adsorption capacity of Enano-$TiO_2$ [15]. However, the potential mechanism underlying sediment P adsorption capacity improved by Enano-$TiO_2$ is still

* Corresponding author.
*E-mail addresses:* czyan@iue.ac.cn, zxluo@iue.ac.cn (C. Yan).

0304-3894/$ – see front matter © 2011 Elsevier B.V. All rights reserved.
doi:10.1016/j.jhazmat.2011.06.050

poorly understood. Therefore, it is important to determine how and to what extent the emerging Enano-$TiO_2$ may influence sediment pore surface properties as well as the consequent P adsorption.

The objectives of this study were to explore the effects of Enano-$TiO_2$ on (1) sediment pore surface properties by applying the nitrogen gas adsorption–desorption method, and (2) the P adsorption capacity on sediment through batch experiments. The information from this study would determine (1) the extent of Enano-$TiO_2$ affecting the particle microstructure of sediment, (2) its potential mechanisms underlying sediment adsorption capacity, and (3) the environmental risk of Enano-$TiO_2$ in aquatic system.

## 2. Materials and methods

### 2.1. Materials

Enano-$TiO_2$ was purchased from Wanjing New Material Company (Hangzhou City, Zhejiang Province, China) with an anatase phase purity of 99.9%, a specific surface area of 202.3 $m^2\ g^{-1}$ and an average particle size of 20 nm. A Enano-$TiO_2$ stock solution (1 $g\ L^{-1}$) was prepared by the following procedures: first to suspend the nanoparticles in a Erlenmeryer flask using ultrapure water, sonicate at 33 W (Sonics Vibra Cell™, model VCX 130, USA) for 10 min, then add dispersion stabilizers (Sodium Polyacrylate, 0.05%) to the dispersion, and finally sonicate the nanoparticles in dispersion with an ultrasound energy of 33 W for 10 min. The size distribution of Enano-$TiO_2$ particles in stock solution was determined using a Laser Particle Size Analyzer (Mastersizer 2000, Marlven, Ltd. UK). The average particle size of Enano-$TiO_2$ particles was $93 \pm 10$ nm.

Ultrapure water was used throughout the experiment. All other chemical reagents were of analytical-reagent grade. Laboratory equipments and containers were dipped in 25% (v/v) $HNO_3$ solution for at least 12 h, and rinsed with ultrapure water prior to each use. All equipment used in the experiments was sterilized at 121 °C for 0.5 h.

Sediment samples were collected from the estuarine of Jiulongjiang River in Fujian province, Southern China (24°27′57.13″N, 117°48′31.70″E), in December 2008, and the samples were transported to the laboratory in sealed plastic bags in iceboxes. They were then freeze-dried, sieved through 80-mesh sieve, and stored for analyses. Sediment pH and electrical conductivity were measured in 1:1 and 1:2 (w/v) soil/water suspensions with a Crison GLP 22 pH-meter. Sediment organic matter (OM) was determined using the potassium dichromate method [29]. The pH, electrical conductivity and organic matter content of the samples were $7.11 \pm 0.15$, $6.50 \pm 0.21$ ms/cm and $49.01 \pm 2.2$ g $kg^{-1}$, respectively.

Preparation of Enano-$TiO_2$-polluted sediment samples: aliquots of 1 g sediments (S) were added into series of 100 mL beakers. The fresh Enano-$TiO_2$ stock solutions (10, 25, 50, 75 and 100 mL) were carefully added into the bottles, and then sonicated for 10 min with ultrasound energy of 33 W. The Enano-$TiO_2$ concentrations in sediment samples were 1, 2.5, 5, 7.5, 10 g $kg^{-1}$, which was lower or greater than the possible polluted concentrations (2.5 g $kg^{-1}$) in the sediments [17]. Additionally, the control sediments (1 g, S) were added into series of 100 mL beaker with 25 mL ultrapure water, but not any Enano-$TiO_2$ pollution (0 mg $L^{-1}$). Accordingly, the sediment suspensions polluted with Enano-$TiO_2$ were heat-dried for 24 h in a flask at about 50 °C, and then slightly ground using a mortar to remove coagulation for further experiments.

### 2.2. Nitrogen adsorption–desorption isotherms

Nitrogen adsorption–desorption was conducted at 77.40 K using an ASAP2020 instrument (Micromeritics, U.S.A.). All samples were degassed at 105 °C for 8 h before $N_2$ was allowed to be contacted. In the experiment, $N_2$ was admitted into the cell in an increment manner so that a series of quantities of absorbed nitrogen were derived, resulting an adsorption isotherm. On the opposite direction, nitrogen was removed from the cell after the gas pressure reached the saturation. A desorption isotherm was derived based on a series of measurements.

Specific surface area of all sediment samples was calculated from $N_2$ sorption isotherm by the multipoint BET method and t-Plot method [30]. Similarly, the average pore size of all sediment samples can be evaluated from the pore size distribution using the method proposed by Barrett, Joyner and Halenda (BJH) based on the $N_2$ adsorption–desorption isotherms of all samples [31].

### 2.3. Calculation of surface fractal dimension [28]

The parameter to describe these fractal characteristics is fractal dimension ($D$). Many methods have been proposed to calculate the fractal dimension based on adsorption–desorption isotherms. The recognized methods are particle size method, the fractal BET model, Frenkel–Halsey–Hill (FHH) model, thermodynamic method, etc. Specifically, the FHH model and the thermodynamic model are the most widely used methods because they can be applied in many cases and easily evaluated. The fractal dimension evaluated by thermodynamic method often gives values greater than 3 so that it becomes meaningless.

The typical FHH theory proposed by Frenkel, Halsey and Hill was first established to describe the multi-layer adsorption of gas molecules on a fractal surface. The linear format is

$$\ln\left(\frac{N}{N_m}\right) = \ln(k) - f(D)\ln(-\ln x); \quad (1)$$

where $f(D)$ is a function of the fractal dimension $D$, $N/N_m$ is the relative nitrogen adsorption volume, $x$ is the relative pressure, and $k$ is a constant. Herein, $N$ and $N_m$ are the nitrogen adsorption volume and the maximum nitrogen adsorption volume in the isotherms. The range of the relative pressure is $x > 0.35$. In this case, the plot of $\ln(N/N_m)$ and $\ln[-\ln(x)]$ should yield a straight line with a slope $S = -f(D)$.

Avnir and Jaroniec [32] and Jaroniec [33] brought the fractal dimension $D$ into the Dubinin–Radushkevich isothermal equation which described nitrogen adsorption on a microporous solid surface. They derived the expression

$$f(D) = 3 - D; \quad (2)$$

Pfeifer et al. [34] suggested that Eq. (2) could be appropriate if capillary condensation was the dominant action in the adsorption process. Moreover, Jaroniec [33] and Pfeifer et al. [34] figured out that the FHH equation was suited for micropore adsorption and desorption processes in which capillary condensation was the dominant action [23]. The range of the relative pressure was determined to be $0.7320 < x < 0.9826$ in the adsorption process and $x > 0.35$ in the desorption process. The resulting FHH equation is

$$\ln\left(\frac{N}{N_m}\right) = (D-3)\ln(-\ln x) + C; \quad (3)$$

Generally, the hysteresis loop on the adsorption–desorption isotherms of sediments is often present [28], indicating that capillary condensation occurs when nitrogen is adsorbed by sediment particles and capillary condensation is the dominant action at a wide range of relative pressure. van der Waals force only dominates when the relative pressure $x$ is lower than 0.35 [35].

Therefore, capillary condensation was considered to be the major action to calculate the fractal dimension of sediment using the FHH method based on the $N_2$ adsorption–desorption isotherm. Specifically, the Eqs. (1), (2) and (3) were adopted to calculate the fractal dimensions of sediments.

### 2.4. Batch experiments

As important sediment P adsorption parameters [29], P adsorption maximum ($S_{max}$) and P binding energy ($K$) were used to evaluate the effects of Enano-$TiO_2$ on P adsorption on the sediment using batch experiments. One gram of dry sediment polluted by Enano-$TiO_2$ was placed into a 50 mL Erlenmerer flask, and treated with 20 mL of a $KH_2PO_4$ solution containing 1, 2, 4, 8, 10, 20, 40, or 50 mg P $L^{-1}$ in a 0.01 M $CaCl_2$ matrix. The mixture was sealed with parafilm and shaken at 150 rpm for 24 h, and then filtered through a 0.45 μm nylon membrane. Phosphorus concentrations in the filtrate were measured by a flow injection analyzer (QC8500, LACHAT, USA.). The $S_{max}$ and $K$ were calculated using the Langmuir isotherm according to the methods described in our previous study [29]. Triplicate samples were used in the experiment.

### 2.5. Statistical analysis

The data reported were the means of triplicates, of which the standard error deviation was within 5%. The normality assumption of Pearson correlation analysis was performed using one sample Kolmogorov–Smirnov test. The homogeneity of variance was evaluated, and Duncan's post hoc test was employed to determine the differences observed of specific surface area, average pore size, and surface fractal dimension of sediments samples. All statistical analyses were conducted at a significance level of 0.05. The software of statistical analysis is SPSS 10.0.

## 3. Results and discussion

### 3.1. Sediment $N_2$ adsorption–desorption isotherm

The adsorption on the material surface is a compositional result involving a combination of chemisorption, quasi-chemisorption, physisorption and capillary condensation [36]. The monolayer chemisorption occurs in the adsorption process, but may have no impact on desorption. A hysteresis was exhibited in the adsorption–desorption isotherms (Fig. 1), suggesting that it is necessary to investigated more thorough on the adsorption and desorption processes.

Fig. 1 depicts the adsorption–desorption isotherms for typical sediment samples polluted by Enano-$TiO_2$ with 0, 2.5, 7.5 and 10 g $kg^{-1}$. The horizontal axis indicates the relative nitrogen pressure ($P/P_0$) in the sample cell, while the vertical axis scales the volume of nitrogen adsorbed by unit weight of the sediment. The volume of nitrogen adsorption in the sediment increased with increasing Enano-$TiO_2$ concentration, indicating that the volume was significantly influenced by Enano-$TiO_2$, specifically in greater concentrations (7.5 and 10 g $kg^{-1}$) (Fig. 1). The adsorption isotherms of all sediment samples were characterized as type II isotherm, a typical multi-layer adsorption model for porous materials [37]. The adsorption volume increased sharply when the $N_2$ pressure approached the saturation point because of capillary condensation [37]. The hysteresis loop of these samples was of type B, indicating that these pores are slit-shaped capillaries, which are close to parallel walls [28,37]. Among the capillaries shaped by parallel walls, liquid nitrogen could not form a meniscus interface before the pressure reaches the saturation point so that a rapid rise was present in the adsorption branch when the relative pressure was close to unity. In the desorption branch, however, vaporization soon occurred when the relative pressure approached the efficient radium of the meniscus interface. It is clear that the typical multilayer adsorption model for porous sediment was insignificantly impacted by Enano-$TiO_2$ pollution. Therefore, the sediment pores were still slit-shaped capillaries, which were close to parallel walls.

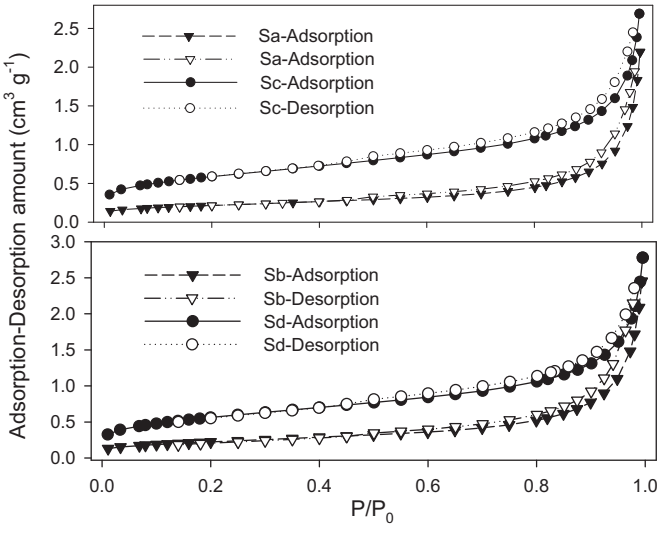


**Fig. 1.** Nitrogen adsorption–desorption isotherms of sediment influenced by Enano-$TiO_2$. (Sa, Sb, Sc, Sd represent the sediment samples contain 0, 2.5, 7.5 and 10 g $kg^{-1}$ Enano-$TiO_2$, respectively.)

### 3.2. Specific surface area and average pore size

The BET Specific surface area ($S_{BET}$) is the total surface area of sediment, which was calculated from $N_2$ sorption isotherms by the multi-BET method [37]. While the external specific surface area ($S_{ext}$) and micropore surface area ($S_{micro}$) were calculated from $N_2$ sorption isotherms by the t-plot method [37]. Specifically, $S_{ext}$ comprises the area of the pore openings and the framework surface between the pore openings on the outside of the sediments [38], while $S_{micro}$ consists of the internal area of the micropore of sediment, which have diameters of <2 nm by definition [39]. The average pore size of sediment polluted by Enano-$TiO_2$ increased significantly with the increase of Enano-$TiO_2$ concentration (Fig. 2). This suggests that Enano-$TiO_2$ particles could fill in the micropores of sediments, and therefore substantially decreased of number of small size micropores, resulting in considerable elevation of average pore size [28,37]. Accordingly, the micropore structure of the sediment was evidently affected by Enano-$TiO_2$ pollution. This could explain why sediment $S_{micro}$ decreased with the increase of Enano-$TiO_2$ concentration (Fig. 2).

Interestingly, the sediment $S_{ext}$ increased remarkably with the increase of Enano-$TiO_2$ concentration (Fig. 2). Similarly, $S_{BET}$ of the Sediments increased significantly with increasing Enano-$TiO_2$ concentration (Fig. 2). This indicated that the substantial decreases of sediment micropores due to the fillings by Enano-$TiO_2$ particles in sediment pores did not significantly decrease $S_{BET}$. In contrast, the attachment of Enano-$TiO_2$ particles to sediment surface considerably enhanced the $S_{ext}$ of the sediments due to high specific surface area of Enano-$TiO_2$, resulting in substantial increase in $S_{BET}$.

### 3.3. Sediment surface fractal dimension

A large number of pores on the sediment surfaces showed some fractal characteristics [28]. The geometric significance of the fractal dimension ($D$) (the value was between 2 and 3 calculated by FHH method) is the fill capacity of sediments pore [37]. The larger the fractal dimension value, the greater the fill capacity [28]. The surface fractal dimension ($D$) of all samples from the three equations in Section 2.3 showed similar decreasing trends with increasing Enano-$TiO_2$ concentration (Table 1).

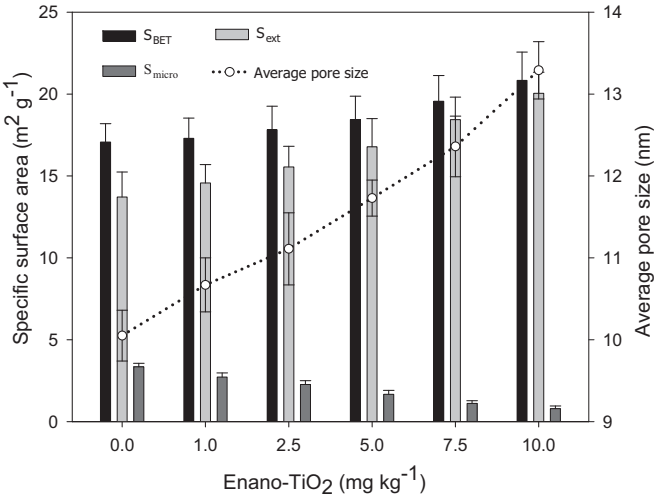


**Fig. 2.** Specific surface area and average pore size of sediment polluted by Enano-$TiO_2$.
Note: $S_{BET}$, total surface area calculated from $N_2$ sorption isotherms by multi-BET method; $S_{micro}$ and $S_{ext}$, micropore and external surface area, respectively, calculated from $N_2$ sorption isotherms by t-plot method.

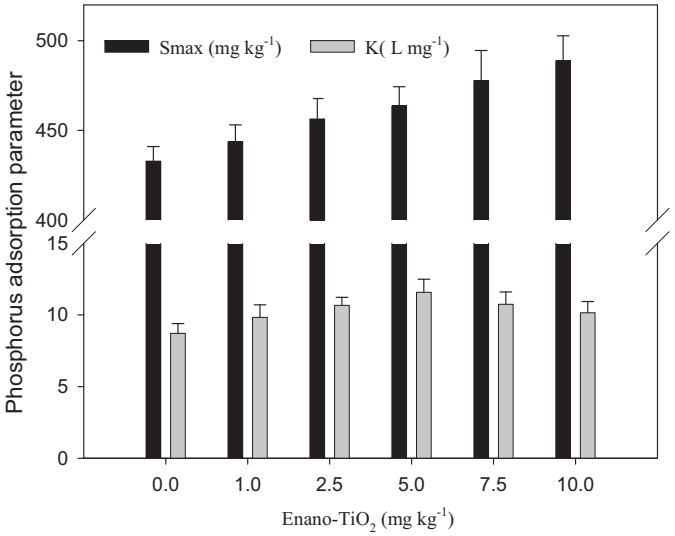


**Fig. 3.** Phosphorus adsorption parameters of sediment polluted by Enano-$TiO_2$.

The fractal dimension offers a more accurate description of the roughness and self-similarity [28]. Slight degree of difference for sediment pores does not change the fractal dimension. The variation of fractal dimensions in Table 1 shows that the Enano-$TiO_2$ pollution has significant impacts on the particle surface microstructure. Therefore, the difference in $D$ value could reflect the influence of Enano-$TiO_2$ on pore surface properties of the sediment. Compared with the $D$ value of the control, the $D$ values of the sediments with Enano-$TiO_2$ were significantly decreased (Table 1), suggesting that the fill capacity of sediment pore could be reduced under the influence of Enano-$TiO_2$ pollution, especially at a relatively high concentration.

### 3.4. Sediment P adsorption

$S_{max}$ is an index measuring the ability of sediment to adsorb P from solution. The higher the $S_{max}$ value, the greater the sediment P adsorption capacity can obtain [29]. In this study, $S_{max}$ values for the sediments increased with increasing Enano-$TiO_2$ concentration, within the range between 432.83 and 488.78 mg $kg^{-1}$ (Fig. 3). $S_{max}$ was positively correlated to $S_{BET}$ and $S_{ext}$ (Table 2). This indicates that the substantial increases of $S_{ext}$ and $S_{BET}$ for sediments due to the attachment of Enano-$TiO_2$ particles to sediments surface could increase P adsorption maximum for the sediments, and therefore enhance the sediment P adsorption capacity. While $S_{max}$ was negatively correlated to $S_{micro}$ and $D$ (Table 2), indicating that the fill in the micropores of sediment could decrease P adsorption maximum, which resulted in the substantially decreases of $S_{micro}$ and $D$. Importantly, even though the fill in the micropores of sediment reduce the sediment P adsorption maximum, the attachment of Enano-$TiO_2$ particles to sediments surface could still increase P adsorption maximum for the sediments. Therefore, Sediment polluted by Enano-$TiO_2$ could improve its P adsorption capacity, which influenced mainly by the attachment of Enano-$TiO_2$ particles to sediments surface.

$K$ represents the ability of a unit of sediment to adsorb P from solution. The higher the $K$ value, the greater the sediment P binding can also obtain [40]. In this study, $K$ value for the sediments initially increased with increasing Enano-$TiO_2$ concentration, and then decreased with increasing Enano-$TiO_2$ concentration, of which the peak value was 11.58 L $mg^{-1}$ at 5.0 mg $L^{-1}$ for Enano-$TiO_2$ (Fig. 3). Noticeably, the increase of Enano-$TiO_2$ does not continuously improve the sediment P binding energy, implying a nonlinear relationship between sediment P binding energy and sediment pore surface properties influenced by Enano-$TiO_2$. This phenomenon can be confirmed from the insignificant correlations between $K$ and any sediment pore surface properties (Table 2).

From the sediment microstructures, the magnitude of $K$ depends on both the $S_{ext}$ and $S_{micro}$ of sediment. The higher the values of $S_{ext}$ and $S_{micro}$, the greater the sediment $K$ can obtain [37]. In this study, the decrease of the $S_{micro}$ resulted in slight decrease of sediment P binding energy with elevated Enano-$TiO_2$ (Fig. 3), even though the $S_{ext}$ was increased considerably by Enano-$TiO_2$. Therefore, $S_{micro}$ have more impacts on sediment $K$ than $S_{ext}$. This indicates that sediment P binding energy relies more on sediment micropore properties probably because P sorbed in sediment micropores is stronger than P sorbed on the sediment external surfaces.

**Table 1**
The surface fractal dimensions of sediment polluted by Enano-$TiO_2$.

| Enano-$TiO_2$ (g $kg^{-1}$) | Surface fractal dimensions ($D$) | | |
|---|---|---|---|
| | Adsorption $x > 0.35$ | Adsorption $0.7320 < x < 0.9826$ | Desorption $x > 0.35$ |
| 0 | 2.588 (0.995) | 2.518 (0.9999) | 2.572 (0.9672) |
| 1 | 2.501 (0.997) | 2.482 (0.9992) | 2.499 (0.9749) |
| 2.5 | 2.487 (0.9920) | 2.446 (0.9995) | 2.447 (0.9650) |
| 5 | 2.426 (0.9950) | 2.419 (0.9993) | 2.394 (0.9620) |
| 7.5 | 2.387 (0.9910) | 2.371 (0.9991) | 2.345 (0.9670) |
| 10 | 2.336 (0.9930) | 2.337 (0.9996) | 2.307 (0.9760) |

*Note*: $x$ indicates the relative nitrogen pressure in nitrogen sorption isotherms; values in parentheses represent the correlation coefficient.

**Table 2**
Correlations between sediment phosphorus adsorption parameters and sediment pore surface properties ($n = 6$).

| | $S_{BET}$ | $S_{ext}$ | $S_{micro}$ | $D$ | | |
|---|---|---|---|---|---|---|
| | | | | Adsorption $x > 0.35$ | Adsorption $0.7320 < x < 0.9826$ | Desorption $x > 0.35$ |
| $S_{max}$ | 0.998** | 0.997** | −0.983** | −0.978** | −0.994** | −0.978** |
| $K$ | 0.539 | 0.560 | −0.634 | −0.617 | −0.559 | −0.659 |

*Note*: ** represent the significant level < 0.01; $S_{BET}$, total surface area calculated from $N_2$ sorption isotherms by multi-BET method; $S_{micro}$ and $S_{ext}$, micropore and external surface area, respectively, calculated from $N_2$ sorption isotherms by t-plot method; $D$, surface fractal dimension.

### 3.5. Implication for environment risk

Clearly, the extensive application of Enano-$TiO_2$ around the world would introduce increasing amount of nano-$TiO_2$ into the environment, resulting in substantial quantity of nano-$TiO_2$ inevitably sinking in aquatic sediments [15,16]. The experimental results of the present study indicate that sediment pore surface properties play pivotal roles in sediment P adsorption. The attachment of Enano-$TiO_2$ particles to sediment surfaces was found to significantly enhance the $S_{BET}$ and $S_{ext}$, thereby increase sediment P adsorption maximum ($S_{max}$). Similar study also showed that Enano-$TiO_2$ could improve sediment P adsorption capacity, possibly due to its larger specific surface area [15]. Therefore, once sediments are polluted with Enano-$TiO_2$, they may accumulate more pollutants such as P, As, etc. resulting in more severe pollution for itself [15,41].

In parallel, it is also found that sediment P binding energy relies more on sediment micropore properties, suggesting that P sorbed in sediment micropores is stronger than P sorbed on sediment external surfaces. The fill of Enano-$TiO_2$ particles into the micropores of the sediments could cause slight decrease in sediment P binding energy ($K$). Subsequently, the strength of P adsorption in the sediments would be reduced substantially due to the decrease of sediment $K$. This indicates that the sorbed P in sediments would be easily released because of the decreased P binding energy of the sediments with elevated Enano-$TiO_2$. In turn, Enano-$TiO_2$ makes P sorbed in sediment easily released when such sediment is re-suspended on disturbance, even through other physicochemical conditions are not changed. Since sediment polluted with Enano-$TiO_2$ may accumulate more pollutants, Enano-$TiO_2$ would be thus cause aggravated endogenous pollution in water if such sediment was re-suspended on disturbance [15], subsequently posing potential risk to the ecosystem [42,43].

## 4. 4 Conclusions

To the best of our knowledge, the study is the first to provide evidence of the regulation or disturbance to sediment physicochemical properties (specifically, pore surface properties) influenced by engineered nanomaterials. Significantly, Enano-$TiO_2$ has great impact on sediment pore surface properties. Interestingly, the attachment of Enano-$TiO_2$ particles to sediment surfaces could increase sediment P adsorption maximum ($S_{max}$), and the fill of Enano-$TiO_2$ particles into the micropores of sediments could cause slight decrease in sediment P binding energy ($K$). Although currently nanomaterials are not regarded as contaminants, the potential risks associated with nanomaterials indicate that water environment management may face the future challenge of the behaviors of sediment that has been contaminated with nanomaterials. Engineered titania nanomaterials (Enano-$TiO_2$) is one of the most widely used nanomaterials. The potential of regulation or disturbance to the physicochemical behavior and processes in environmental media caused by Enano-$TiO_2$ can provide insights into the environmental risks of other similar nanomaterials. Therefore, these preliminary results of Enano-$TiO_2$ are important for further understanding the potential risks of similar nanomaterials in the aquatic environment.

## Acknowledgements

The authors gratefully acknowledge research funding supported by the Knowledge Innovation Program of Chinese Academy of Sciences (project no. KZCX2-YW-Q02-04) and National Nature Science Foundation of China (project no. 41001331 and 20807033) and helpful comments from the anonymous reviewers.

## References

[1] A. Nel, T. Xia, L. Madler, N. Li, Toxic potential of materials at the nano level, Science 311 (2006) 622–627.
[2] A.D. Maynard, R.J. Aitken, T. Butz, V. Colvin, K. Donaldson, G. Oberdorster, M.A. Philbert, J. Ryan, A. Seaton, V. Stone, S.S. Tinkle, L. Tran, N.J. Walker, D.B. Warheit, Safe handling of nanotechnology, Nature 444 (2006) 267–269.
[3] B. Nowack, T.D. Bucheli, Occurrence, behavior and effects of nanoparticles in the environment, Environ. Pollut. 150 (2007) 5–22.
[4] Y. Ju-Nam, J.R. Lead, Manufactured nanoparticles: an overview of their chemistry, interactions and potential environmental implications, Sci. Total Environ. 400 (2008) 396–414.
[5] T. Hofmann, F. von der Kammer, Estimating the relevance of engineered carbonaceous nanoparticle facilitated transport of hydrophobic organic contaminants in porous media, Environ. Pollut. 157 (2009) 1117–1126.
[6] L.K. Adams, D.Y. Lyon, P.J. Alvarez, Comparative eco-toxicity of nanoscale $TiO_2$, $SiO_2$, and ZnO water suspensions, Water Res. 40 (2006) 3527–3532.
[7] S. Bastian, W. Busch, D. Kuhnel, A. Springer, T. Meissner, R. Holke, S. Scholz, M. Iwe, W. Pompe, M. Gelinsky, A. Potthoff, V. Richter, C. Ikonomidou, K. Schirmer, Toxicity of tungsten carbide and cobalt-doped tungsten carbide nanoparticles in mammalian cells in vitro, Environ. Health Perspect. 117 (2009) 530–536.
[8] E. Navarro, A. Baun, R. Behra, N.B. Hartmann, J. Filser, A.J. Miao, A. Quigg, P.H. Santschi, L. Sigg, Environmental behavior and ecotoxicity of engineered nanoparticles to algae, plants, and fungi, Ecotoxicology 17 (2008) 372–386.
[9] A.B. Boxall, K. Tiede, Q. Chaudhry, Engineered nanomaterials in soils and water: how do they behave and could they pose a risk to human health? Nanomedicine (London, England) 2 (2007) 919–927.
[10] A.A. Koelmans, B. Nowack, M.R. Wiesner, Comparison of manufactured and black carbon nanoparticle concentrations in aquatic sediments, Environ. Pollut. 157 (2009) 1110–1116.
[11] J. Labille, J. Brant, Stability of nanoparticles in water, Nanomedicine–UK 5 (2010) 985–998.
[12] X. Quan, X. Zhao, S. Chen, H.M. Zhao, J.W. Chen, Y.Z. Zhao, Enhancement of p,p'-DDT photodegradation on soil surfaces using $TiO_2$ induced by UV-light, Chemosphere 60 (2005) 266–273.
[13] K. Nagaveni, G. Sivalingam, M.S. Hegde, G. Madras, Photocatalytic degradation of organic compounds over combustion-synthesized nano-$TiO_2$, Environ. Sci. Technol. 38 (2004) 1600–1604.
[14] R.J. Aitken, M.Q. Chaudhry, A.B.A. Boxall, M. Hull, Manufacture and use of nanomaterials: current status in the UK and global trends, Occup. Med.–Oxford 56 (2006) 300–306.
[15] Z.X. Luo, Z.H. Wang, Q.Z. Li, Q.K. Pan, C.Z. Yan, Effects of titania nanoparticles on phosphorus fractions and its release in resuspended sediments under UV irradiation, J. Hazard. Mater. 174 (2010) 477–483.
[16] M.A. Kiser, P. Westerhoff, T. Benn, Y. Wang, J. Perez-Rivera, K. Hristovski, Titanium nanomaterial removal and release from wastewater treatment plants, Environ. Sci. Technol. 43 (2009) 6757–6763.
[17] Z.X. Luo, Z.H. Wang, Q.Z. Li, Q.K. Pan, C.Z. Yan, F. Liu, Spatial distribution, electron microscopy analysis of titanium and its correlation to heavy metals: occurrence and sources of titanium nanomaterials in surface sediments from Xiamen Bay, China, J. Environ. Monit. 13 (2011) 1046–1052.
[18] T. Masciangioli, W.X. Zhang, Environmental technologies at the nanoscale, Environ. Sci. Technol. 37 (2003) 102A–108A.
[19] X. Zhang, H. Sun, Z. Zhang, Q. Niu, Y. Chen, J.C. Crittenden, Enhanced bioaccumulation of cadmium in carp in the presence of titanium dioxide nanoparticles, Chemosphere 67 (2007) 160–166.

[20] S.B. Lovern, J.R. Strickler, R. Klaper, Behavioral and physiological changes in *Daphnia magna* when exposed to nanoparticle suspensions (titanium dioxide, nano-C60, and C60HxC70Hx), Environ. Sci. Technol. 41 (2007) 4465–4470.
[21] M.R. Wilson, L. Foucaud, P.G. Barlow, G.R. Hutchison, J. Sales, R.J. Simpson, V. Stone, Nanoparticle interactions with zinc and iron: implications for toxicology and inflammation, Toxicol. Appl. Pharmacol. 225 (2007) 80–89.
[22] M. Bernardeschi, P. Guidi, V. Scarcelli, G. Frenzilli, M. Nigro, Genotoxic potential of $TiO_2$ on bottlenose dolphin leukocytes, Anal. Bioanal. Chem. 396 (2010) 619–623.
[23] M. Hajnos, L. Korsunskaia, Y. Pachepsky, Soil pore surface properties in managed grasslands, Soil Till Res. 55 (2000) 63–70.
[24] S.R. Carpenter, N.F. Caraco, D.L. Correll, R.W. Howarth, A.N. Sharpley, V.H. Smith, Nonpoint pollution of surface waters with phosphorus and nitrogen, Ecol. Appl. 8 (1998) 559–568.
[25] J. Kopacek, J. Borovec, J. Hejzlar, K.U. Ulrich, S.A. Norton, A. Amirbahman, Aluminum control of phosphorus sorption by lake sediments, Environ. Sci. Technol. 39 (2005) 8784–8789.
[26] Y. Wang, Z.Y. Shen, J.F. Niu, R.M. Liu, Adsorption of phosphorus on sediments from the Three-Gorges Reservoir (China) and the relation with sediment compositions, J. Hazard. Mater. 162 (2009) 92–98.
[27] S.R. Wang, X.C. Jin, H.C. Zhao, F.C. Wu, Phosphorus release characteristics of different trophic lake sediments under simulative disturbing conditions, J. Hazard. Mater. 161 (2009) 1551–1559.
[28] H.W. Fang, M.H. Chen, Z.H. Chen, Surface pore tension and adsorption characteristics of polluted sediment, Sci. China Ser. G 51 (2008) 1022–1028.
[29] Z.X. Luo, B. Zhu, J.L. Tang, T. Wang, Phosphorus retention capacity of agricultural headwater ditch sediments under alkaline condition in purple soils area, China, Ecol. Eng. 35 (2009) 57–64.
[30] K. Yang, D.H. Lin, B.S. Xing, Interactions of humic acid with nanosized inorganic oxides, Langmuir 25 (2009) 3571–3576.
[31] E.P. Barrett, L.G. Joyner, P.P. Halenda, The determination of pore volume and area distributions in porous substances. 1. Computations from nitrogen isotherms, J. Am. Chem. Soc. 73 (1951) 373–380.
[32] D. Avnir, M. Jaroniec, An isotherm equation for adsorption on fractal surfaces of heterogeneous porous materials, Langmuir 5 (1989) 1431–1433.
[33] M. Jaroniec, Evaluation of the fractal dimension from a single adsorption-isotherm, Langmuir 11 (1995) 2316–2317.
[34] P. Pfeifer, Y.J. Wu, M.W. Cole, J. Krim, Multilayer adsorption on a fractally rough-surface, Phys. Rev. Lett. 62 (1989) 1997–2000.
[35] P. Tang, N.Y.K. Chew, H.K. Chan, J.A. Raper, Limitation of determination of surface fractal dimension using N-2 adsorption isotherms and modified Frenkel-Halsey-Hill theory, Langmuir 19 (2003) 2632–2638.
[36] R. Desai, M. Hussain, D.M. Ruthven, Adsorption of water-vapor on activated alumina. 1. Equilibrium behavior, Can. J. Chem. Eng. 70 (1992) 699–706.
[37] S. Lowell, J.E. Shields, Powder Surface Area and Porosity, 3rd ed., Chapman & Hall, London, 1991.
[38] Z.Q. Liu, M.F. Ottaviani, L. Abrams, X.G. Lei, N.J. Turro, Characterization of the external surface of silicalites employing electron paramagnetic resonance, J. Phys. Chem. A 108 (2004) 8040–8047.
[39] M.E. Hodson, Micropore surface area variation with grain size in unweathered alkali feldspars: implications for surface roughness and dissolution studies, Geochim. Cosmochim. Acta 62 (1998) 3429–3435.
[40] D.R. Smith, B.E. Haggard, E.A. Warnemuende, C. Huang, Sediment phosphorus dynamics for three tile fed drainage ditches in Northeast Indiana, Agric. Water Manage. 71 (2005) 19–32.
[41] H.W. Sun, X.Z. Zhang, Q. Niu, Y.S. Chen, J.C. Crittenden, Enhanced accumulation of arsenate in carp in the presence of titanium dioxide nanoparticles, Water Air Soil Pollut. 178 (2007) 245–254.
[42] R. Kaegi, A. Ulrich, B. Sinnet, R. Vonbank, A. Wichser, S. Zuleeg, H. Simmler, S. Brunner, H. Vonmont, M. Burkhardt, M. Boller, Synthetic $TiO_2$ nanoparticle emission from exterior facades into the aquatic environment, Environ. Pollut. 156 (2008) 233–239.
[43] M.R. Wiesner, G.V. Lowry, P. Alvarez, D. Dionysiou, P. Biswas, Assessing the risks of manufactured nanomaterials, Environ. Sci. Technol. 40 (2006) 4336–4345.